Electronic Supplementary Material (ESI) for Nanoscale.

Supplementary Information

Imaging and quantification of charged domain walls in $BiFeO_3$

Marco Campanini,*[a] Elzbieta Gradauskaite,[b] Morgan Trassin,[b] Di Yi,[c] Pu Yu,[d] Ramamoorthy Ramesh,[e] Rolf Erni,[a] and Marta D. Rossell[a]

[a.] *Electron Microscopy Center, Empa, Swiss Federal Laboratories for Materials Science and Technology, Ueberlandstr. 129, 8600 Dübendorf, Switzerland*
[b.] *Laboratory for Multifunctional Ferroic Materials, ETHZ, 8093 Zürich, Switzerland*
[c.] *State Key Laboratory of New Ceramics and Fine Processing, School of Materials Science and Engineering, Tsinghua University, Beijing 100084, China.*
[d.] *State Key Laboratory of Low Dimensional Quantum Physics and Department of Physics, Tsinghua University, Beijing 100084, China.*
[e.] *Department of Materials Science and Engineering and Department of Physics, UC Berkeley, Berkeley, California 94720, USA.*

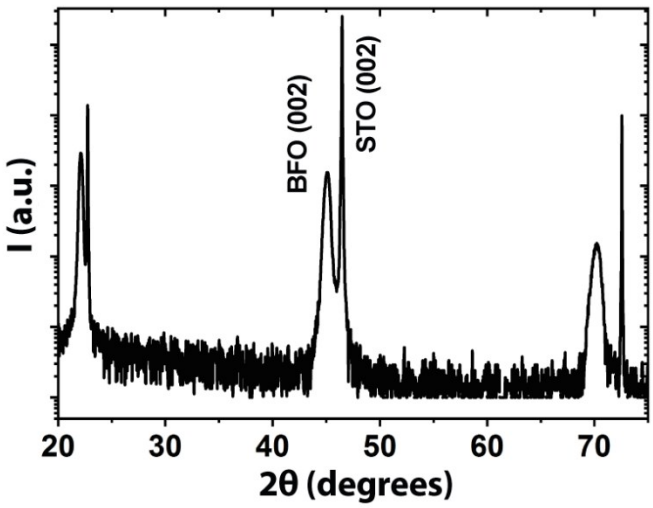

Figure S1. XRD pattern of the $BiFeO_3/La_{0.7}Sr_{0.3}MnO_3/SrRuO_3$ heterostructure grown on a (001)-oriented STO substrate. The diffraction peaks correspond to a fully *c*-oriented film.

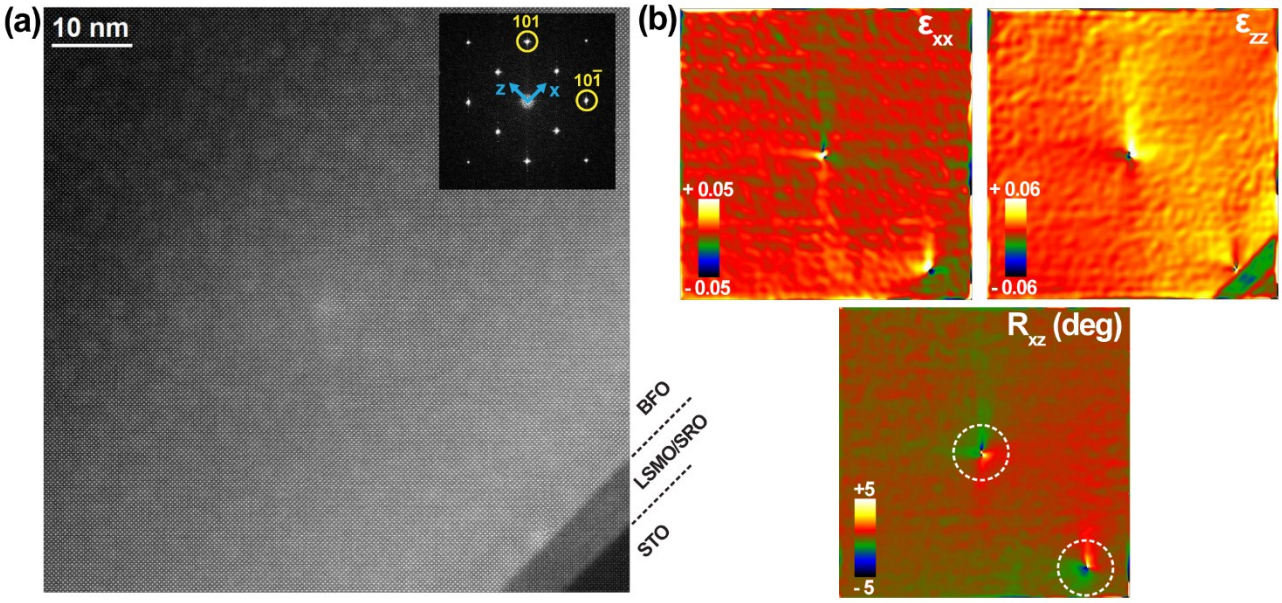

Figure S2. (a) High-resolution HAADF image of the $BiFeO_3/La_{0.7}Sr_{0.3}MnO_3/SrRuO_3$/STO heterostructure. The inset shows the power spectrum of the image. (b) Strain analysis by Geometric Phase Analysis (GPA) method. The ε_{xx} and ε_{zz} maps demonstrate that the $BiFeO_3$ film is in a strain-relaxed state. The strain relaxation is achieved by the formation of edge dislocation pairs. One pair is marked in the rotation map (R_{xz}) by the two dashed circles.

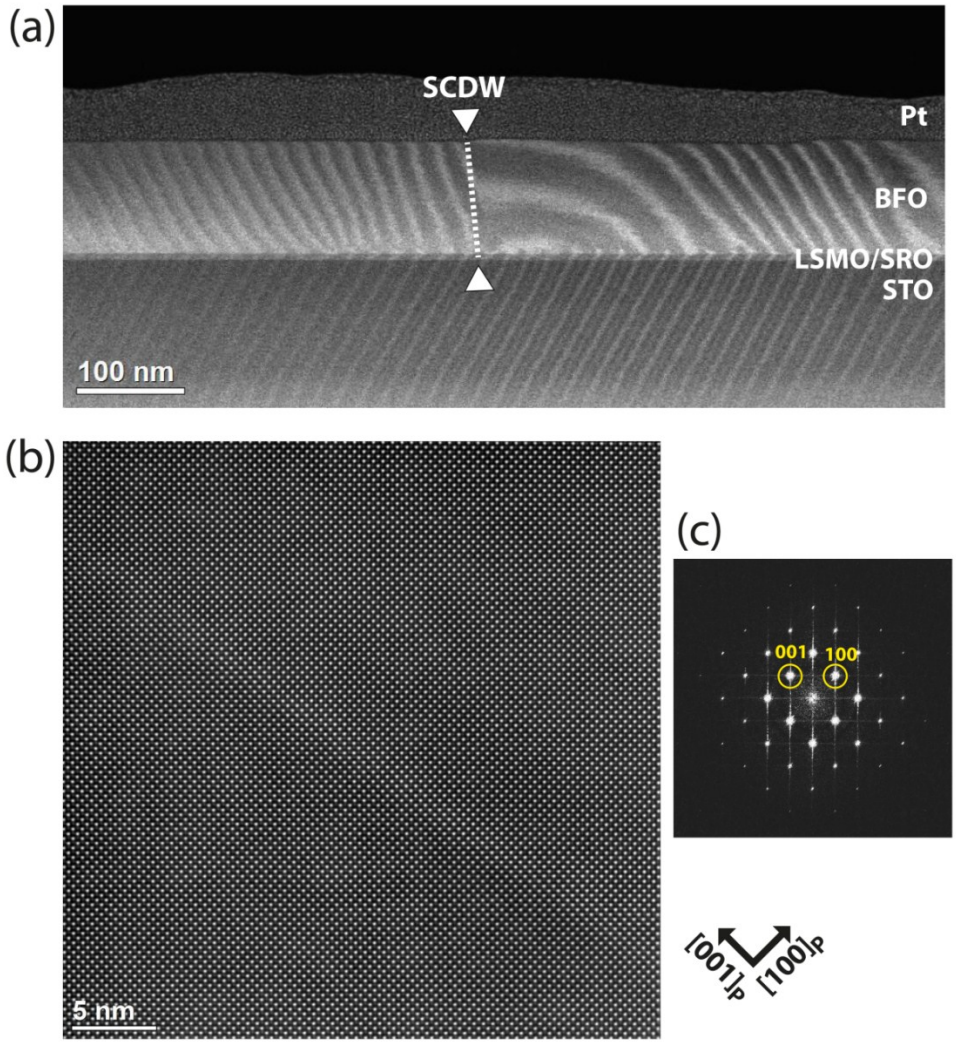

Figure S3. (a) Medium resolution HAADF-STEM image of the cross sectional sample of the multilayer heterostructure $BiFeO_3/La_{0.7}Sr_{0.3}MnO_3/SrRuO_3$. The Moire fringes due to the raster scan periodicity help in detecting the 109° T-T DW. (b) High-resolution HAADF-STEM image of the 109° T-T DW. The DW is easily visible thanks to its brighter contrast. The main crystallographic directions of the pseudocubic setting are given. (c) Power spectrum of the image showing that there is no significant crystal misorientation for the two domains separated by the 109° DW.

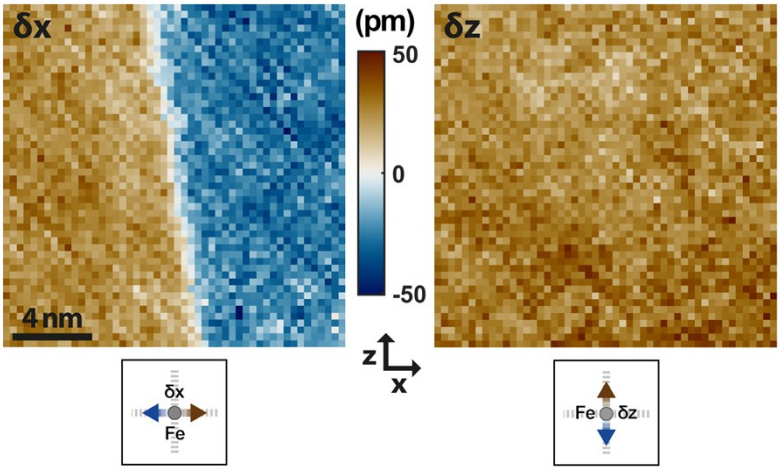

Figure S4. Maps of the in-plane (δx) and out-of-plane (δz) atomic displacement components of the B-site cation used for the calculation of the ferroelectric polarization as presented in Fig. 2 of the main text. Note that the ferroelectric polarization is antiparallel to the Fe displacement.

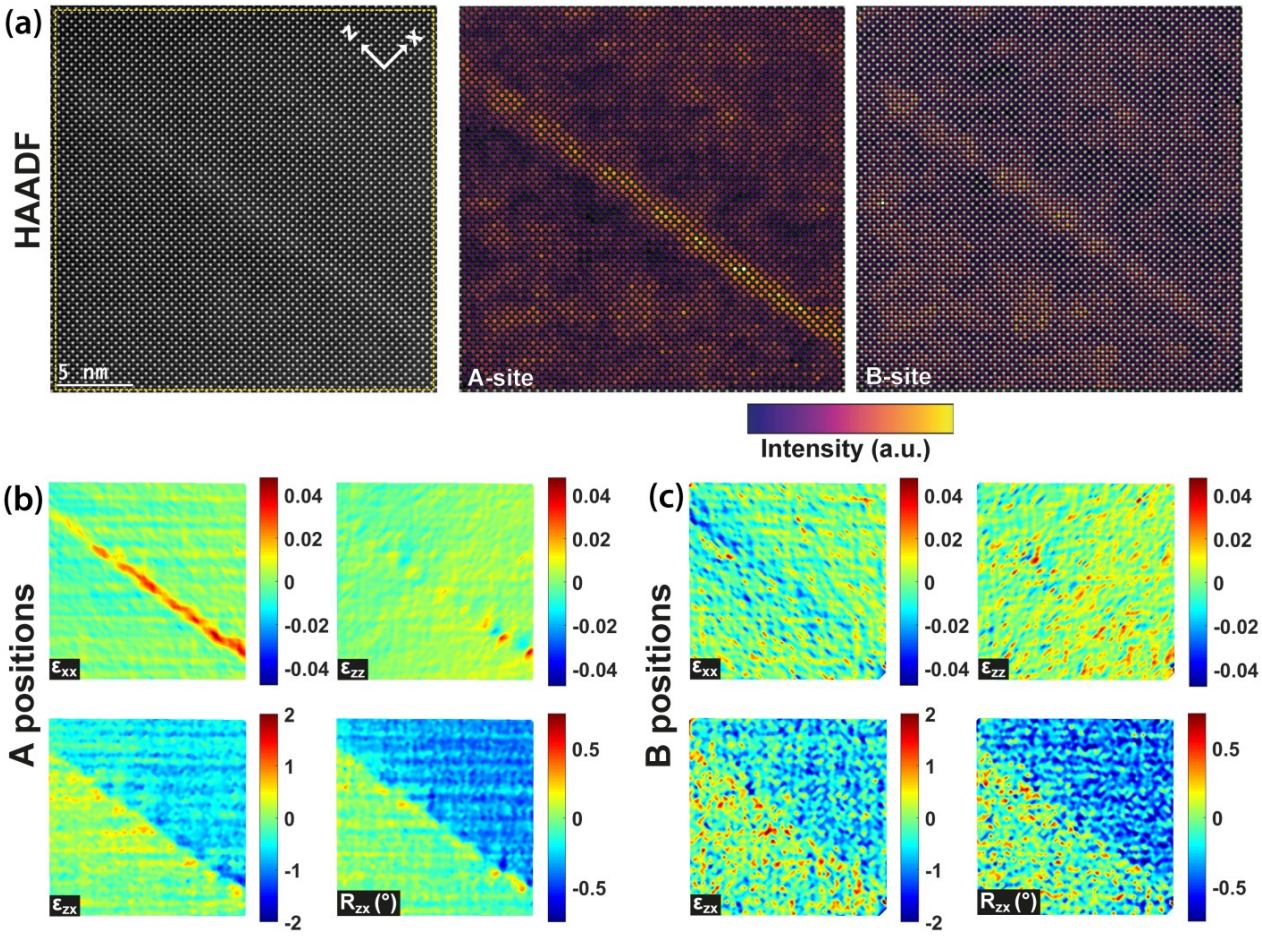

Figure S5. Intensity and strain analysis performed by Peak-Pair analysis (PPA), for the image shown in Figure S1). (a) HAADF-STEM signal and analysis of the peak intensities for the A- and B-site columns of the perovskite cell. (b, c) Strain maps for the A and B cations, respectively. The axes shown in (a) gives the principal directions for the strain analysis. The area of the HAADF signal where the strain analysis was performed is marked by the yellow dashed box on the HAADF signal.

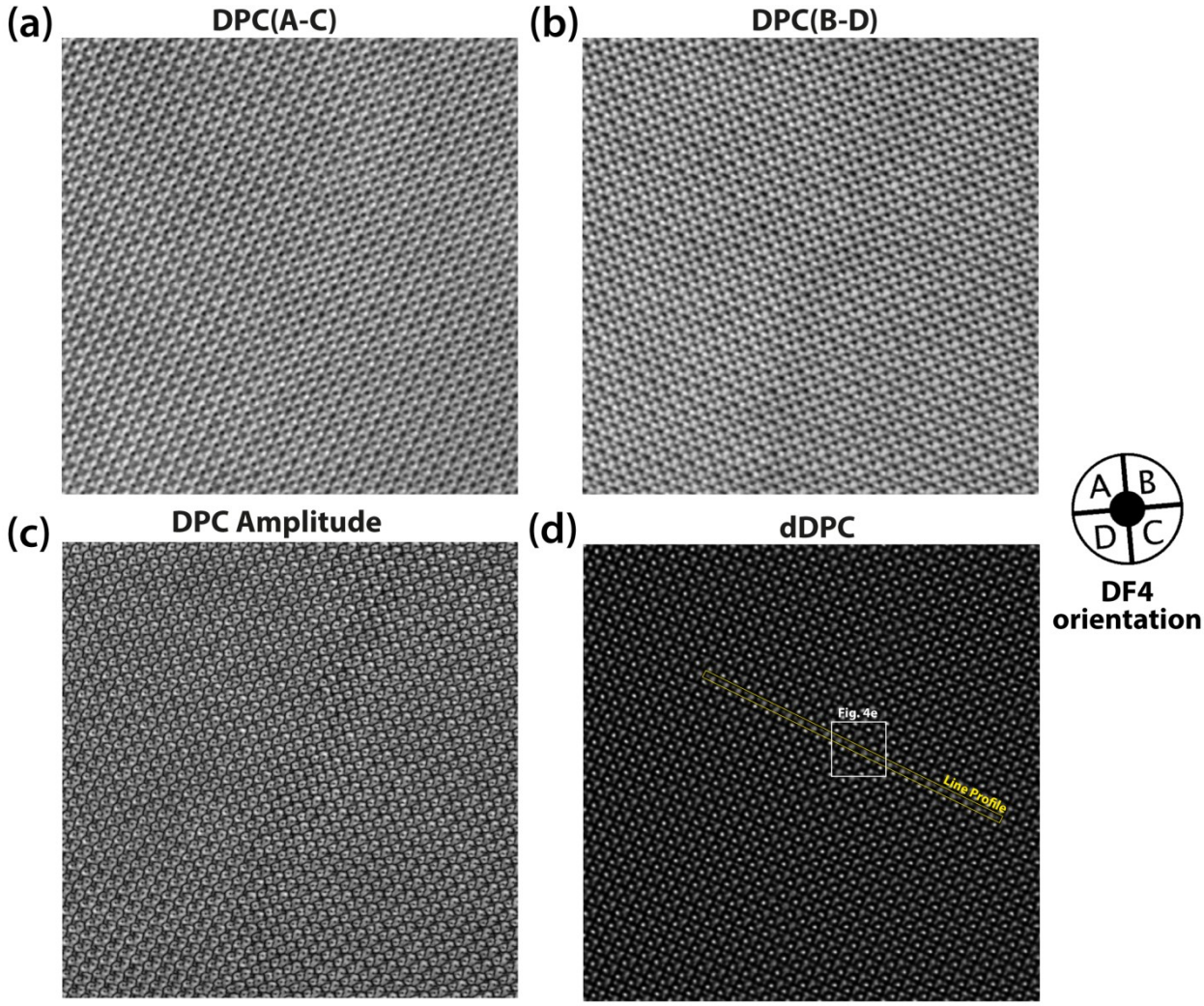

Figure S6. (a, b) DPC-STEM images obtained subtracting the signal of opposite pairs of quadrants, i.e. (A-C) and (B-D). These two signals are related to the projected electric field components. (c) DPC amplitude calculated as the modulus of the DPC vector image. (d) dDPC signal obtained differentiating the DPC vector image.

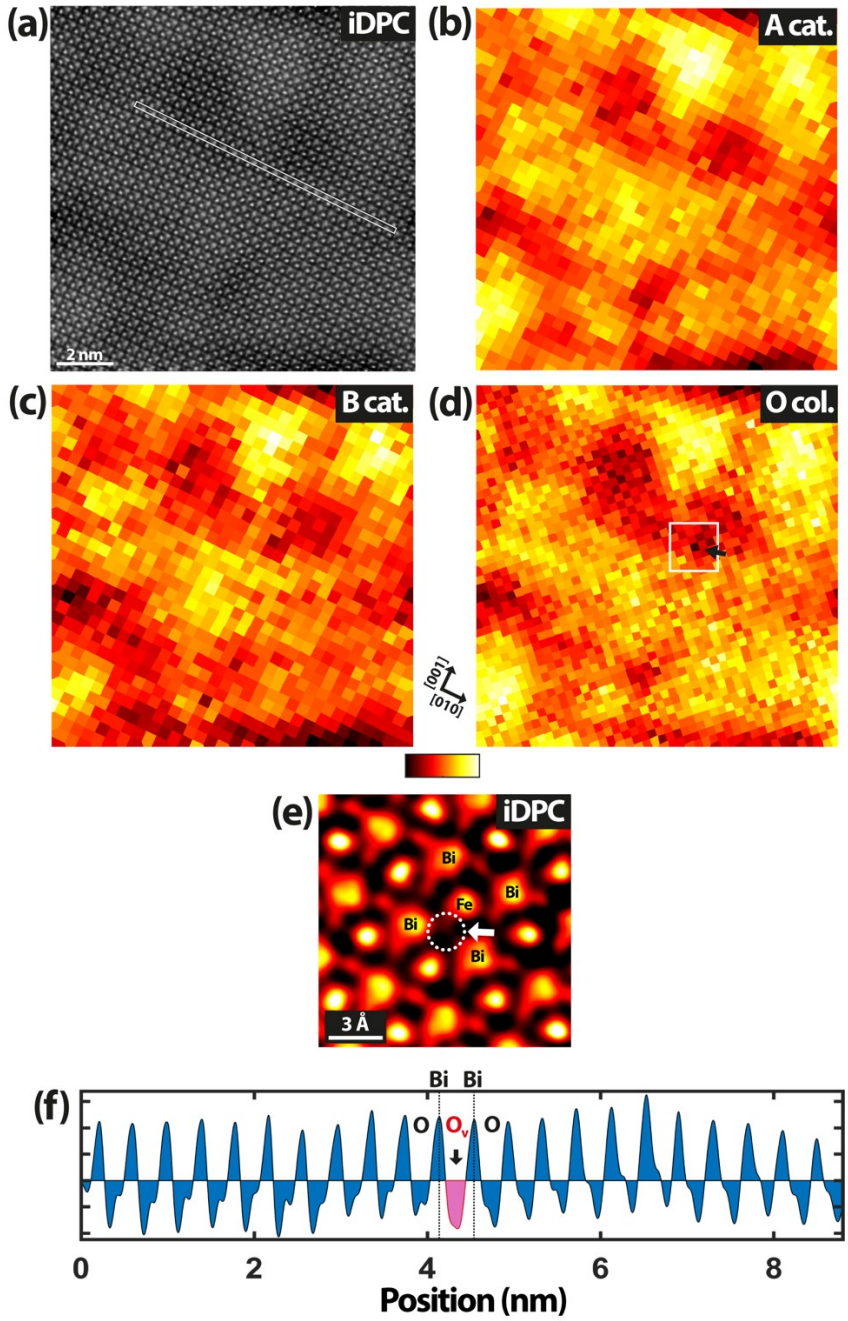

Figure S7. (a) iDPC signal obtained from the data shown in Fig S6. (b)-(d) Maps of the fitted intensities for the A-site and B-site cations and O columns, respectively. The field of view of the maps corresponds to the one of Fig. 4 b-d. The low frequency features appear to be the same in the three maps, highlighting the significant role of specimen surface contamination on the iDPC signal. (e) Magnified view of the portion marked by the white box in (d). The white dashed circle highlights the position of the highly vacant O column. (f) Line profile - taken along the rectangular selection in (a) - similar to the one shown in Fig. 4f, but obtained for the iDPC signal.